Single molecules in soft matter : a study of biomolecular conformation, heterogeneity and plasmon enhanced fluorescence

Yuan, H.

6 Large enhancement of single-molecule fluorescence near individual gold nanorods

Abstract –Plasmonic nanostructures can create strongly enhanced local fields when excited at their plasmon resonances. Utilizing such strong fields, fluorescence of single molecules near a plasmonic nanostructure can be enhanced. The fluorescence enhancement factor, however, depends on many parameters such as the field enhancement, the position of the fluorophore with respect to the nanostructure, and their spectral overlap. Here, we study the fluorescence enhancement of single molecules (crystal violet) near individual gold nanorods (GNRs). Allowing the dye molecules to diffuse in a highly viscous liquid (glycerol), we found fluorescence enhancement factors up to one thousand times with individual GNRs.

A part of this chapter has been published:
H. Yuan, S. Khatua, P. Zijlstra, M. Yorulmaz, and M. Orrit, "Thousand-fold enhancement of single-molecule fluorescence near a single gold nanorod", *Angew. Chem. Int. Ed.* **52** (2013) 1217–1221.

6.1 Introduction

Optical detection of single molecules mostly relies on their fluorescence because of the high contrast of this technique against background. Since their invention in the early 1990's, single-molecule fluorescence microscopy and spectroscopy have spread to many fields in chemistry, physics and biology, and have provided a unique access to nanometer scales [13]. New developments have yielded insight into a wide range of phenomena, including the dynamics of enzymes [25, 194] and the subwavelength arrangement of cellular components [195, 196]. A primary requirement of this technique is that the emission rate of the molecules under study must be as high as possible. However, an overwhelming majority of the strongly absorbing molecules (called chromophores) fluoresce only weakly and hence are not detectable by conventional single-molecule fluorescence techniques. Prominent examples are metal complexes and many biological chromophores, such as hemes. Herein, we will show how fluorescence enhancement by a plasmonic nanoparticle may be harnessed to overcome this limitation and extend single-molecule studies to weakly emitting species.

The enhancement of single-molecule fluorescence near a plasmonic nanoparticle may arise from two factors. (i) In contrast to dielectrics, metals support a collective response of conduction electrons, which can concentrate the optical field in the vicinity of a particle. Excitation can be enhanced by this high local field, particularly close to tips or protrusions [71, 174, 197, 198]. This lightning rod effect is further amplified by resonance if the excitation frequency coincides with a surface plasmon resonance (SPR) of the particle. The excitation enhancement (ϕ_{ex}) can be written as $|E^2|/|E_o^2|$, where $|E^2|$ is the near-field intensity and $|E_o^2|$ is the intensity without the presence of GNRs. (ii) The rate of emission by a fluorophore can also be enhanced by a similar antenna effect [199]. This Purcell effect can be seen as an enhanced density of optical states accessible for decay for a dipole at the position of the molecule, or, equivalently, as enhancement of the transition dipole moment by electric currents in the nanoparticle antenna [200]. The Purcell effect may not only change the intensity of the emission, but also its spectral shape, fluorescence lifetime, and quantum yield. As metals also enhance non-radiative decay rates, they may quench fluorescence. Therefore, the balance between enhancement and quenching depends on the exact position of the fluorophore with respect to the nanoparticle. The emission enhancement (ϕ_{em}) can be described by η/η_o, where η is the effective quantum yield in presence of GNRs and η_o is the intrinsic quantum yield of the dye. Therefore, the overall fluorescence enhancement (ϕ_f) can be written as a product of excitation enhancement (ϕ_{ex})

and emission enhancement (ϕ_{em}):

$$\phi_f = \frac{|E^2|\eta}{|E_o^2|\eta_o} \tag{6.1}$$

By the late 1990's, a number of near-field optics experiments had shown the existence of distinct regimes of enhancement and quenching in the interaction of a single molecule with a metal tip [201]. At distances less than 5 nm, molecular excitations are efficiently dissipated in the metal by a mechanism similar to Förster transfer. At intermediate distances (10 nm-50 nm), however, currents in the metal can actually enhance the radiating dipole and boost emission by the optical antenna effect. Later measurements on single gold nanospheres by the groups of Sandoghdar and Novotny have confirmed these two regimes [202, 203], although field enhancement by a single sphere is rather modest (only a factor 3 or so). More recently, researchers have put molecules in interaction with lithographically fabricated nanostructures designed for strong field enhancement. Prominent examples are the directional Yagi-Uda antenna by Van Hulst's group [204] and the bowtie nano-antenna by Hecht's [205] and Moerner's [206] groups. In the latter work, a fluorescence intensity enhancement of up to 1340 was demonstrated for a molecule with a low quantum yield [206].

Enhancing the fluorescence by a lithographically made metal nanostructure has a number of drawbacks. (i) The structures are often difficult and expensive to fabricate. (ii) Even more importantly, as the gold films produced by standard evaporation or sputtering techniques are polycrystalline, their plasmon resonances are significantly broadened and weakened. In contrast to those structures, chemically synthesized gold nanorods are easy to make. Their single-crystalline structure generates narrow and intense plasmon resonances [174, 207]. Theory predicts fluorescence enhancements of up to several thousand times at the tips of gold nanorods [208, 209]. Experimental realizations, so far, have lagged far behind this prediction, with a maximum single-molecule fluorescence enhancement of only 40 fold, as achieved by Fu *et al* [210]. The main hurdle is the accurate positioning of a single fluorophore in the region of the highest field enhancement.

In this work, we report large enhancements of single-molecule fluorescence of more than a thousand times by chemically synthesized gold nanorods. The reported enhancement is one to two orders of magnitude higher than in previous reports [210,211]. We have achieved such high enhancements by (a) selecting a dye with significant overlap with the surface plasmon of nanorods, (b) allowing single dye molecules to diffuse slowly through the near-field of a single

nanorod and (c) using laser excitation that is close to the surface plasmon resonance of GNRs. As individual fluorophores explore the field profile near the particle, a molecule will occasionally diffuse through the most favorable position where the enhancement is maximum. Monitoring the fluorescence with a high enough time resolution, we determine the maximum enhancement by analyzing bursts in fluorescence timetraces. The maximum enhancement factors show clear dependence on excitation wavelengths and nanorods' plasmon resonances.

6.2 Materials and methods

Gold nanorods with average dimensions of 25 nm × 60 nm were synthesized by the seed-mediated growth method [180]. The scanning electron microscope (SEM) image is shown in figure 6.1 (a). The longitudinal plasmon resonance of these nanorods is approximately at 650 nm. Figure 6.1 (b) shows a bulk extinction spectrum of these nanorods dispersed in glycerol. For our single particle studies, the nanorods, coated with cetyl-trimethylammonium bromide (CTAB), were isolated on a glass coverslip by spin coating from a water suspension. After spin coating, the additional CTAB was removed by washing 2-3 times with MilliQ water and by subsequent UV/Ozone treatment for 30 minutes.

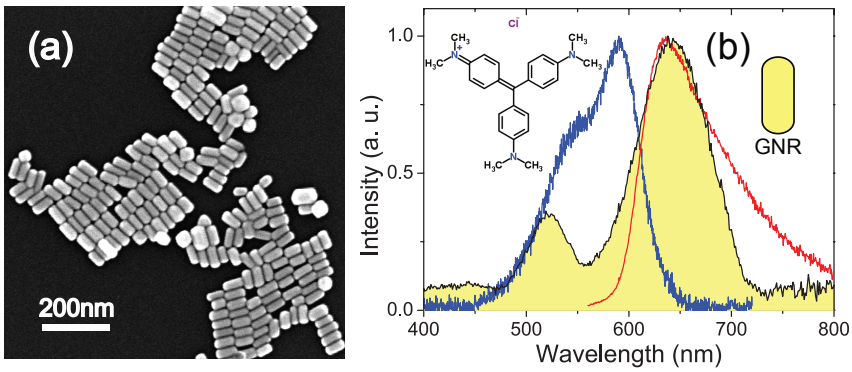

Figure 6.1: SEM image of a drop of gold nanorod suspension dried on a silicon chip. On average, the nanorods are 25(±4) nm wide and 58(±7) nm long. (b) Extinction spectra of gold nanorods dispersed in glycerol (shaded area), absorption (blue) and fluorescence (red) spectra of CV in glycerol. Inset: chemical structure of CV.

We selected crystal violet (CV) molecules for the enhancement study. CV has its absorption maximum at 596 nm and its emission maximum at 640 nm,

ensuring a significant overlap with the SPR of the nanorods, as shown in figure 6.1 (b). CV has a low fluorescence yield (QY) of 0.019 [212]. It has been previously reported that fluorescence enhancement depends on the QY of the dye and higher enhancements can be achieved for lower QY [72, 206, 208, 209]. Low QYs also offer better contrast against the fluorescence background of unenhanced molecules.

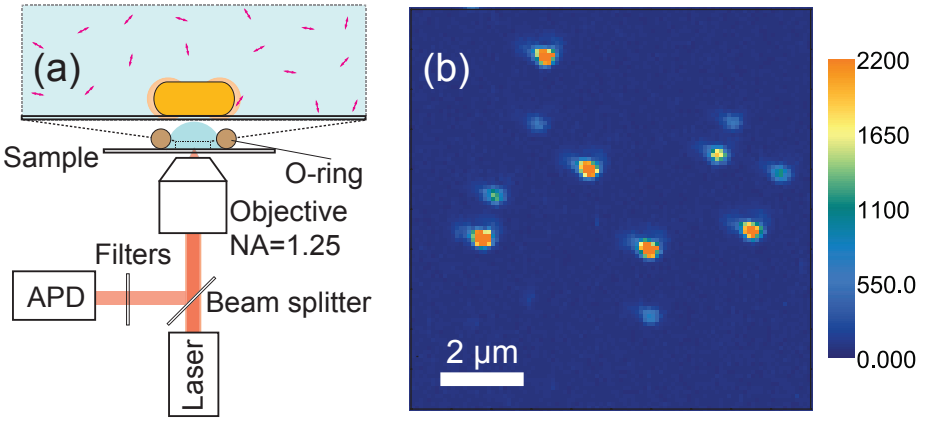

Figure 6.2: (a) A simplified scheme of the experimental setup. The small double-sided arrows represent single CV molecules diffusing in solution and the yellow body represents a nanorod. (b) A photoluminescence image of the nanorods isolated on a glass coverslip and immersed in glycerol doped with 100 nM CV. A circularly polarized 633 nm laser was used as the excitation source. The excitation intensity was 5 kW/cm^2. The image consists of 120×120 pixels with an integration time of 10 ms/pixel.

Confocal microscopy was performed on our home-built microscope, assembled on an inverted optical microscope. The details of the setup are described elsewhere [14, 70]. Briefly, a circularly polarized Helium-Neon laser (633 nm or 594 nm) or an Ar-ion laser (514 nm) is used as excitation source. An oil immersion objective with a numerical aperture (NA) of 1.25 focused the excitation laser to a diffraction-limited spot (about 300 nm diameter). The red-shifted fluorescence from the sample was collected by the same objective and was separated from the excitation laser by a notch filter (removing 514 nm, 594 nm or 633 nm, according to the excitation wavelength). Fluorescence was detected by an avalanche photo-diode (APD) or a liquid-nitrogen-cooled CCD. Images were acquired by scanning the sample across the focus with a piezo-scanning stage. Fluorescence lifetimes of CV molecules are measured using a time-correlated single photon counting setup (Pico-Quant). A 635 nm pulsed laser

(less than 100 ps pulse width) was used as excitation source. An avalanche photodiode (MPD) was used as detector. Using NIM timing output from the MPD, we could improve the instrument response function (IRF) to ∼120 ps.

Figure 6.2 (b) shows a typical photoluminescence image of the nanorods isolated on a glass coverslip and immersed in glycerol doped with 100 nM CV. The excitation wavelength was 633 nm. Each bright spot in figure 6.2 (b) arises from photoluminescence of a single nanorod. This is confirmed by measuring a photoluminescence spectrum of each bright spot. We used 514 nm laser excitation to record the luminescence spectra of the nanorods. The 514 nm excitation was preferred because it is energetically far from the longitudinal SPR of the nanorods (see figure 6.1 b) and thus enabled us to record the full nanorod emission spectrum. We found approximately 90% (35 out of 40 spots) of the bright spots to stem from single nanorods, evidenced by their narrow spectral width and Lorentzian line shape. An example spectrum is shown in the inset of figure 6.3. We note that scattering spectra are more commonly used in the literature to check for single nanorods, however, as we have recently shown that scattering spectra closely resemble luminescence spectra, the latter can be used as well [70]. Figure 6.2 (b), recorded with excitation at 633 nm, shows a large variation of the photoluminescence intensity among the bright spots in the image. This intensity variation is due to volume differences from nanorod to nanorod and most importantly to the different positions of their surface plasmon resonance with respect to the excitation.

6.3 Results and discussion

Fluorescence timetraces taken on individual nanorods show fluorescence bursts. Figure 6.3 (a) shows a typical fluorescence intensity trace taken on a single nanorod whose spectrum is shown in the inset of figure 6.3 (b). The large background signal of the fluorescence trace, ∼700 counts in 10 ms, comes from all the CV molecules present in the focal volume of the excitation laser as well as from some intrinsic luminescence of the nanorod. The contribution of CV molecules can be deduced from a fluorescence trace taken under the same experimental conditions but on an area without a nanorod. Figure 6.4 (a) shows such a trace with an average count of ∼170 per 10 ms bin time. At the given CV concentration of 100 nM, we expect approximately 60 molecules in the focal volume at any given time (considering a focal volume of 1 fL). From this, we estimate on average ∼2-3 counts/molecule/10 ms. It is interesting to compare this signal to the intrinsic photoluminescence of the nanorod. This nanorod appears to be about two orders of magnitude brighter (∼500 counts

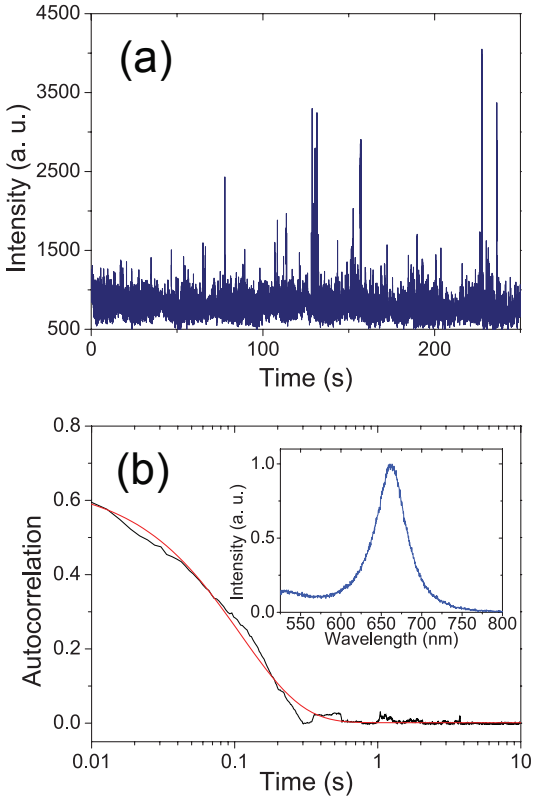

Figure 6.3: (a) A fluorescence intensity time trace taken on a single gold nanorod immersed in glycerol doped with 100 nM CV molecules. (b) The luminescence spectrum of this nanorod is shown in the inset. The Lorentzian lineshape of the plasmon resonance confirms the presence of a single nanorod. Autocorrelation curve (black) of the fluorescence bursts shown in (a). A single exponential fit (red) yields a correlation time of 120 ms.

per 10 ms) than an individual CV molecule under our experimental conditions, even though the nanorods are known to have a much lower luminescence QY (10^{-5} or less) [70, 213] than CV ($\sim 10^{-2}$). This high brightness is explained by the very high absorption cross section of the nanorod at resonance ($\sim 10^3\,\mathrm{nm}^2$) compared to the absorption cross section of a single CV molecule ($\sim 10^{-2}\,\mathrm{nm}^2$).

To verify that the observed fluorescence bursts are from CV molecules, we performed blank experiments where we measured fluorescence timetraces of single gold nanorods under identical conditions (633 nm excitation with same power density of $5\,\mathrm{kW/cm}^2$) but immersed in pure glycerol. We did not observe

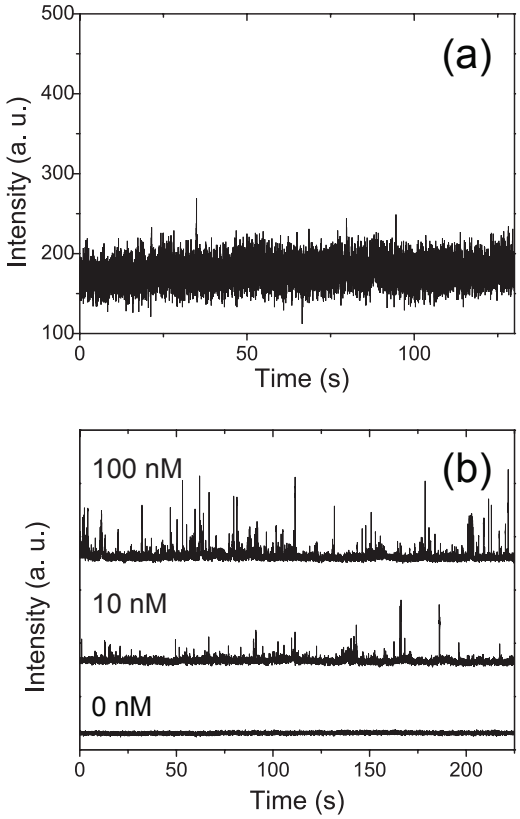

Figure 6.4: (a) A fluorescence timetrace recorded on a solution of 100 nM CV in glycerol, with no nanorods present. We observe only 2-3 very weak fluorescence bursts which could be due to some impurity present in the solution. The excitation power density is 5 kW/cm^2 at 633 nm. (b) Fluorescence timetraces recorded on single gold nanorods at different CV concentrations. When there was no CV in the sample, no fluorescence bursts were observed in the fluorescence time-trace (black). When we increased the CV concentration to 10 nM, some bursts (about 30 bursts) were seen in the fluorescence trace-trace (red). More than 200 bursts appeared in the time trace (blue) when we further increased the CV concentration to 100 nM. The excitation power density is 5 kW/cm^2 at 633 nm.

any fluorescence burst, as shown in the example trace (0 nM) in figure 6.4 (b). Moreover, we recorded fluorescence timetraces on single gold nanorods immersed in glycerol solutions with different concentrations of CV. Figure 6.4 (b) shows example timetraces taken on single gold nanorods in 10 nM and 100 nM CV solutions in glycerol. We can see an occurrence of fluorescence bursts

approximately an order of magnitude larger (∼30 bursts to ∼200 bursts in a 225 s time window) in the solution with higher CV concentration. It clearly demonstrates the dependence of burst frequencies on CV concentrations.

The previous experiments show that the fluorescence bursts must be due to enhanced fluorescence of CV molecules. Such fluorescence bursts are also observed in standard fluorescence correlation spectroscopy (FCS) where single fluorophores diffuse through the focal volume of the excitation laser. These experiments, however, are performed at very low concentrations (typically tens of pM to 1 nM) so that only one molecule (or very few ones) is present in the focal volume at any given time [214, 215]. In this experiment, we used a CV concentration of 100 nM, corresponding to approximately 60 molecules in the focal volume. We therefore do not expect any significant fluctuation of fluorescence in a confocal fluorescence time trace. This is confirmed by the absence of fluctuations in a fluorescence time trace recorded from a 100 nM CV solution in glycerol in the absence of gold nanorods (figure 6.4 a). We also rule out the possibility of aggregates of CV, as these molecules carry a net positive charge and form very stable solutions in polar solvents. We did not observe any significant shift of the absorption maximum or change in the shape of absorption spectra of CV dissolved in glycerol as a function of concentration (up to 30 μM) and time (6 hours). Finally, we note a slight decrease in background fluorescence after some minutes of exposure time. This can be attributed to photobleaching in the focal volume.

Moreover, the fluorescence intensity bursts were predominantly polarized along the long axis of the nanorod, as shown in figure 6.5. After a polarizing beam splitter, the fluorescence photons collected from the sample can be separated into two parts of orthogonal polarizations (horizontal and vertical polarizations) and be detected at two APDs. Photoluminescence images of the same GNR at two orthogonal polarizations are shown in figure 6.5 (a) and (b). The GNR shows a very bright photoluminescence intensity with horizontal polarization, which is 4 times larger than that with vertical polarization. This observation indicates the GNR's long axis is almost in parallel with the horizontal direction. The fluorescence timetraces at these two polarizations are shown in figure 6.5 (c). The fluorescence bursts with horizontal polarization are much stronger than those with vertical polarization. These results confirm that the polarization of fluorescence bursts strongly depends on the GNR's orientation. It further confirms that the fluorescence enhancement is caused by the presence of a nanorod.

The maximum intensity of the fluorescence burst shown in figure 6.3 (a) is 4050 counts/10 ms, corresponding to an increase of 3350 counts/10 ms over the

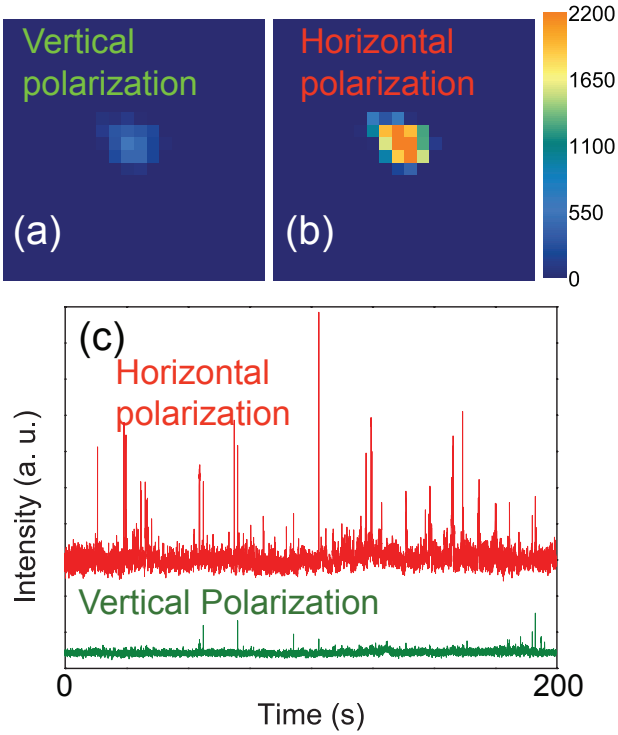

Figure 6.5: (a) Photoluminescence image of a GNR with vertical polarization. (b) The photoluminescence image on the same GNR with horizontal polarization. (c) The fluorescence timetraces recorded on the same GNR with both polarizations.

background signal of 700 counts/10 ms (fluorescence from background CV and nanorod). This increase is due to the enhanced fluorescence from one single CV molecule. Based on the fact that each CV molecule (when not enhanced) produces ∼3 counts per 10 ms, this burst leads to a calculated fluorescence enhancement factor of ∼1120. We can rule out the possibility that this enhancement is caused by more than one CV molecule because at the given concentration of 100 nM, less than 0.001 CV molecules are present in the near field of a nanorod ($\sim 10^4\,\mathrm{nm}^3$). We repeated the fluorescence enhancement study on 21 individual nanorods and found large variations in the maximum fluorescence enhancement among them. The lowest maximum enhancement we found was 165 and the highest one 1150.

The large fluorescence enhancements also allow us to perform a fluorescence correlation study at a concentration of CV of 100 nM. Typical FCS

studies are done at much lower fluorophore concentrations (10 pM to 1 nM). Figure 6.3 (b) shows the autocorrelation curve (black) of the fluorescence bursts from the time trace shown in figure 6.3 (a). A single exponential fit (red) to the autocorrelation curve yields a correlation time of 120 ms. We repeated this procedure for 21 other nanorods and found that most of them show a single exponential decay with an average correlation time of 100±40 ms. For a few nanorods, we also see an additional slower component with correlation time up to several seconds. Using the bulk viscosity of glycerol, we can estimate a single CV molecule to spend a few ms in the near field of the nanorod. This time is almost two orders of magnitude shorter than the average correlation time recovered from the autocorrelation curves. This discrepancy might indicate significant sticking of CV to the nanorod or to the substrate, followed by bleaching, as found in a previous report [72]. More work is needed to clarify this point.

Fluorescence enhancement also depends on the excitation wavelength. Excited close to resonance, a GNR can create a very strong near-field intensity. On the contrary, the near-field intensity around the GNR becomes much weaker under off-resonance excitation. Figure 6.6 (a) shows the fluorescence traces measured on the same GNR (SPR at 650 nm) but with different excitation wavelengths (633 nm and 594 nm). Applying the same excitation power, the GNR under 633 nm excitation shows much brighter fluorescence bursts than under 594 nm excitation. The different fluorescence enhancements observed on the same dye and GNR under different excitation wavelengths clearly demonstrate the effect of excitation enhancement.

Emission enhancement can be demonstrated by measuring the fluorescence lifetimes. Figure 6.6 (b) shows a small section of a fluorescence trace measured on a GNR (SPR at 650 nm) under pulsed excitation at 635 nm. Several fluorescence bursts of different intensities can be identified. We select two bursts (highlighted in blue and dark yellow color and by dashed boxes) as examples. The fluorescence decays of these two bursts are shown in figure 6.6 (c). Without the presence of GNRs, CV in glycerol shows a fluorescence lifetime of 1 ns (black squares). The burst of lower intensity (dark yellow circles) shows a fluorescence lifetime of 450 ps. The other burst of higher intensity (blue dots) shows an even shorter fluorescence lifetime that can hardly be resolved by our instrument with a 120 ps response function (red solid curve). The shortened fluorescence lifetimes observed in these bursts indicate enhancement of decay rates, which may arise from enhanced radiative decay rate and/or nonradiative decay rate. Measuring on the whole trace on this GNR, we correlate the fluorescence lifetimes of each burst with its fluorescence intensity, as shown

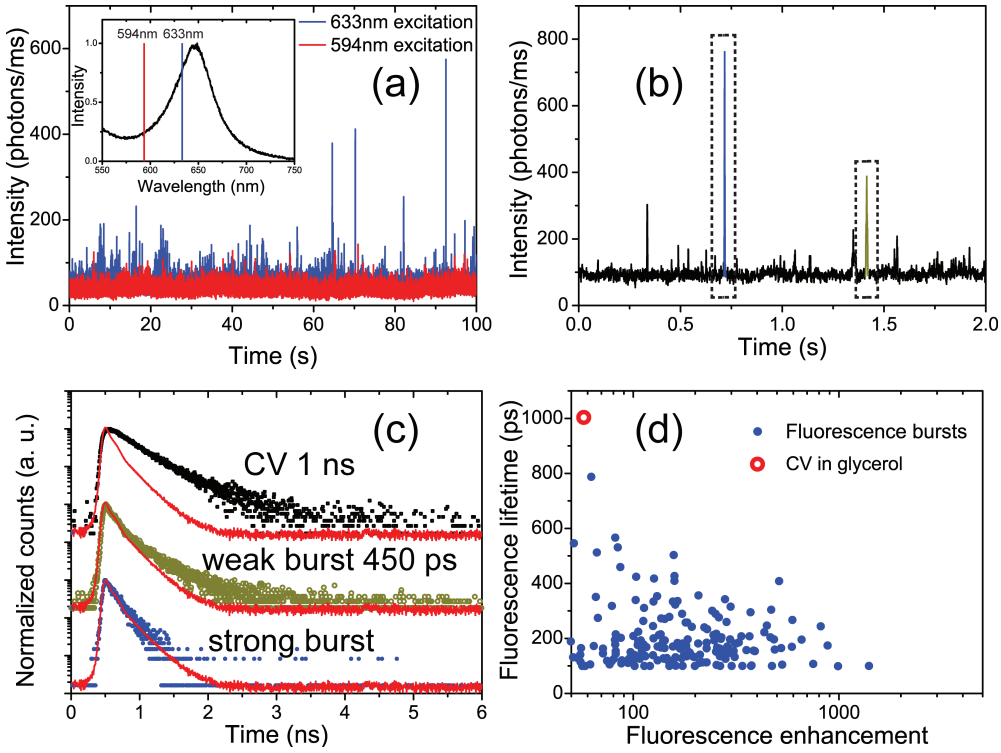

Figure 6.6: (a) The fluorescence traces measured on the same GNR (SPR at 650 nm) under laser excitation at different wavelengths. Inset: the photoluminescence spectrum of the individual GNR. The blue trace is taken under 633 nm excitation. The red trace is taken under 594 nm excitation. The excitation power densities are both 5 kW/cm^2. (b) A small section of a fluorescence trace recorded under 635 nm pulsed excitation. (c) The fluorescence decay of bulk CV in glycerol (black squares) and fluorescence decays measured on two enhanced bursts. The blue dots show the fluorescence decay of the strong burst highlighted in (b). The dark yellow circles show the fluorescence decay of the weak burst highlighted in (b). The red solid curves show the instrumental response function (IRF). (d) The correlation between the fluorescence lifetime of each burst and its intensity enhancement. The red circle shows the fluorescence lifetime measured on bulk CV in glycerol without the presence of GNRs.

in figure 6.6 (d). We see a general correlation between the shortening of fluorescence lifetime and larger fluorescence enhancement, a fact which is also evident from figure 6.6 (c). We also observe a significant population of data which corresponds to weaker fluorescence enhancements (less than 200 times) but their fluorescence lifetimes are also much shorter than that of bulk CV.

We associate these events with quenching of the fluorescence due to the close proximity between the nanorod and CV molecules. In our experiment, CV molecules are free to diffuse and thus can come close enough to the GNR for quenching to take place.

Therefore, the large fluorescence enhancement reported in this work results from both excitation enhancement and emission enhancement by the nanorod. At resonance, the field enhancement factor in the near field of the rod, resulting from a combination of lightning rod effect and of plasmonic resonance, can exceed 30 [197,208]. This factor can lead to intensity enhancements of ∼1000 for the excitation rate, and/or to a similar factor for the spontaneous emission rate, depending on the respective spectral overlaps of the excitation line, of the fluorescence band, and of the plasmon resonance. Careful adjustment of the overlap between the surface plasmon resonance of a gold nanorod and the molecular absorption and emission spectra has been predicted from theory to yield fluorescence enhancements of up to several thousand. [208] In our experiment, as fluorescence traces were recorded with a 633 nm laser which is very close to the surface plasmon resonance of the nanorods, we expect a large excitation enhancement. We note that our excitation intensity is rather low (each CV molecule absorbs $\sim 10^6$ photons/s) and even with a maximum excitation enhancement of 1000, the molecule is well below its saturation limit (total decay rate of $10^{11}\,\mathrm{s}^{-1}$) and thus can take the full advantage of the excitation enhancement. Moreover, the emission rate can also be enhanced as the plasmon resonance of the nanorods is close to the fluorescence maximum of the CV molecules (figure 6.1 b). Thus the high enhancement we observe here is most likely a combination of excitation and emission enhancements. The exact contribution of each of these factors will depend on the surface plasmon resonance of each particle and hence the overall enhancement would vary from nanorod to nanorod. Indeed, we observe a broad distribution of enhancement among the different nanorods we have studied. A quantitative estimation, however, requires more experimental and theoretical work.

6.4 Conclusion

In conclusion, we report large fluorescence enhancements of up to one-thousand-fold by chemically synthesized gold nanorods. This large enhancement is achieved by selecting a dye with its absorption and emission very close to the surface plasmon resonance of the nanorods and by measuring the maximum enhancement corresponding to the optimum position of the fluorophore with respect to the nanorod. We demonstrate an application of this large

enhancement to perform correlation spectroscopy at a concentration of fluorophores two orders of magnitude higher (100 nM) than commonly used (10 pM to 1 nM). This promises broader application of fluorescence correlation spectroscopy to many systems, notably in biology, where the analyte concentrations can be very high and cannot be arbitrarily reduced. We note that the enhancement factors reported here are still well below the theoretically predicted maximum values. Further improvements including the use of dyes with a better spectral overlap with the nanorods and a still lower intrinsic quantum yield will be explored in the near future.

Acknowledgements

We thank Ankur Gupta and Prof. Thijs Aartsma for their help in fluorescence lifetime measurements. H. Y., S. K., M. Y. and M. O. acknowledge financial support from the European Research Council (Advanced Grant SiMoSoMa). P. Z. acknowledges financial support from the Netherlands Organization for Scientific Research (Veni Fellowship).